Fig .1- PFTs

Examples of α*(right)* and β PFTs *(left)*. Crystal structure of *S. aureus* α-hemolysin (7AHL). It is a homo-oligomeric heptamer with a 2.2 nm diameter pore lumen and height 10 nm. Crystal structure of an actinoporin fragaceatoxin C (FraC) from sea anemone *(right).* Pore is composed of six subunits with a height of 11 nm. The internal diameter of the water filled lumen is 1.6 nm (4TSY)

Fig.2 Structures of monomer and pore

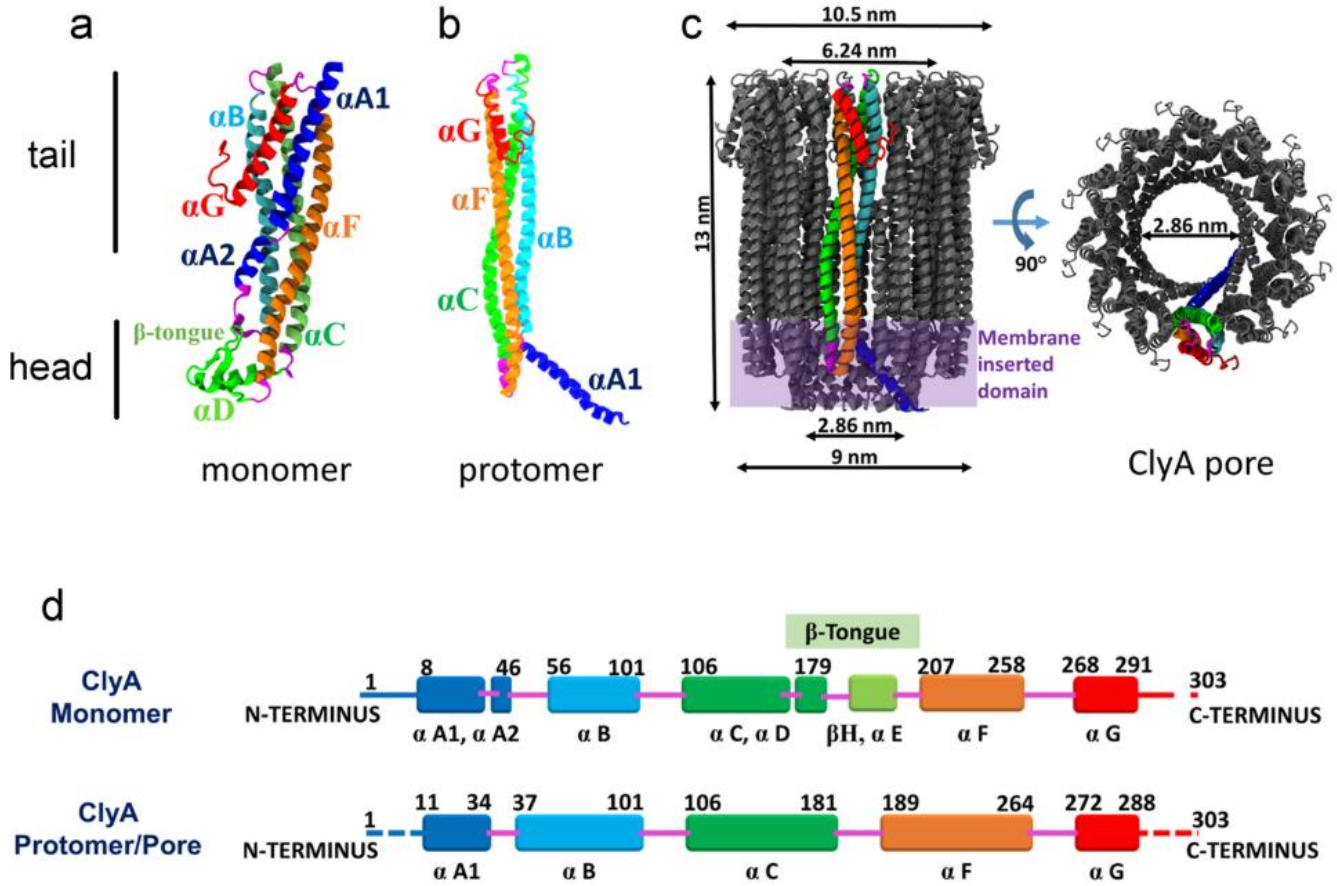

ClyA structures(a) Crystal structure of the monomer (PDB entry 1QOY) color-coded as per the line diagram in panel d. (b) A single protomer from the cytolysin A pore is highlighted and color-coded according to the line diagram in panel d. (c) The cytolysin A pore is shown, and its length, inner diameter, and outer diameter on the cytosolic side as well as the solvent-exposed side are illustrated along with its transmembrane region. (d) Line diagrams of ClyA in its monomeric and protomeric pore integral conformations with the secondary structures color-coded according to Mueller et al. The structurally unresolved C-terminus in the monomer (residues 299−303) and both termini in the protomer (residues 1−7 of the N-terminus and residues 293−303 of the C-terminus) are depicted as dashed lines.

Fig.3 Models of Pore formation

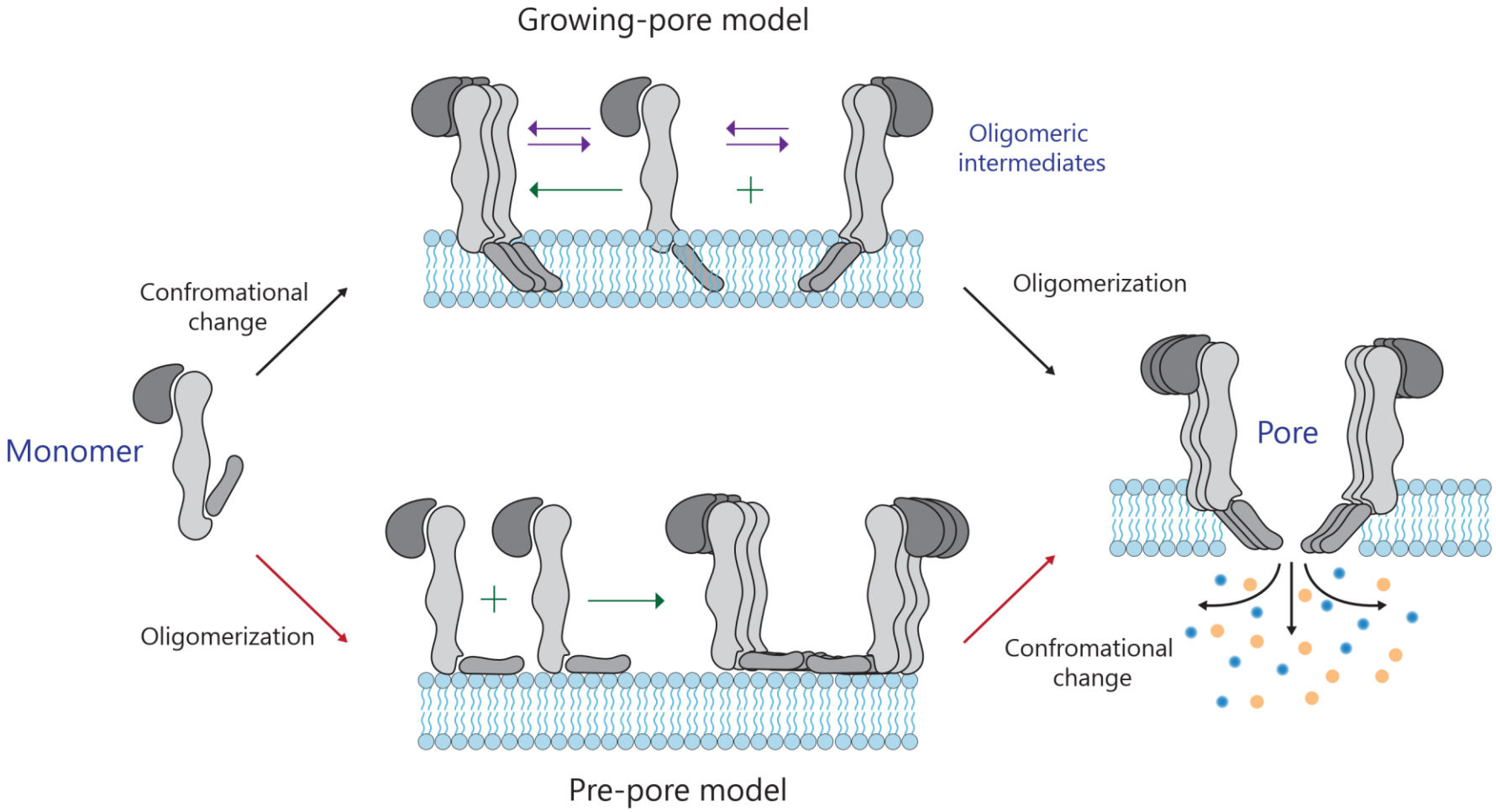

Models for ClyA pore formation. *Top* Growing pore model: ClyA is produced in soluble form and undergoes conformational change with the N-terminus inserting into the membrane. This unit can oligomerize via sequential (green arrow) or non-sequential (purple arrows) to result in formation of the full pore. *Bottom* Pre-pore model: Upon contact with membrane, ClyA binds to the membrane via the β-tongue and subsequently oligomerizes to form a metastable intermediate structure called 'pre-pore', where the N-terminal helix αA is proposed to lie parallel to the membrane surface . Pore is formed after coordinated insertion of αA helices from all protomers into the membrane.

Fig. 4: Structure based model

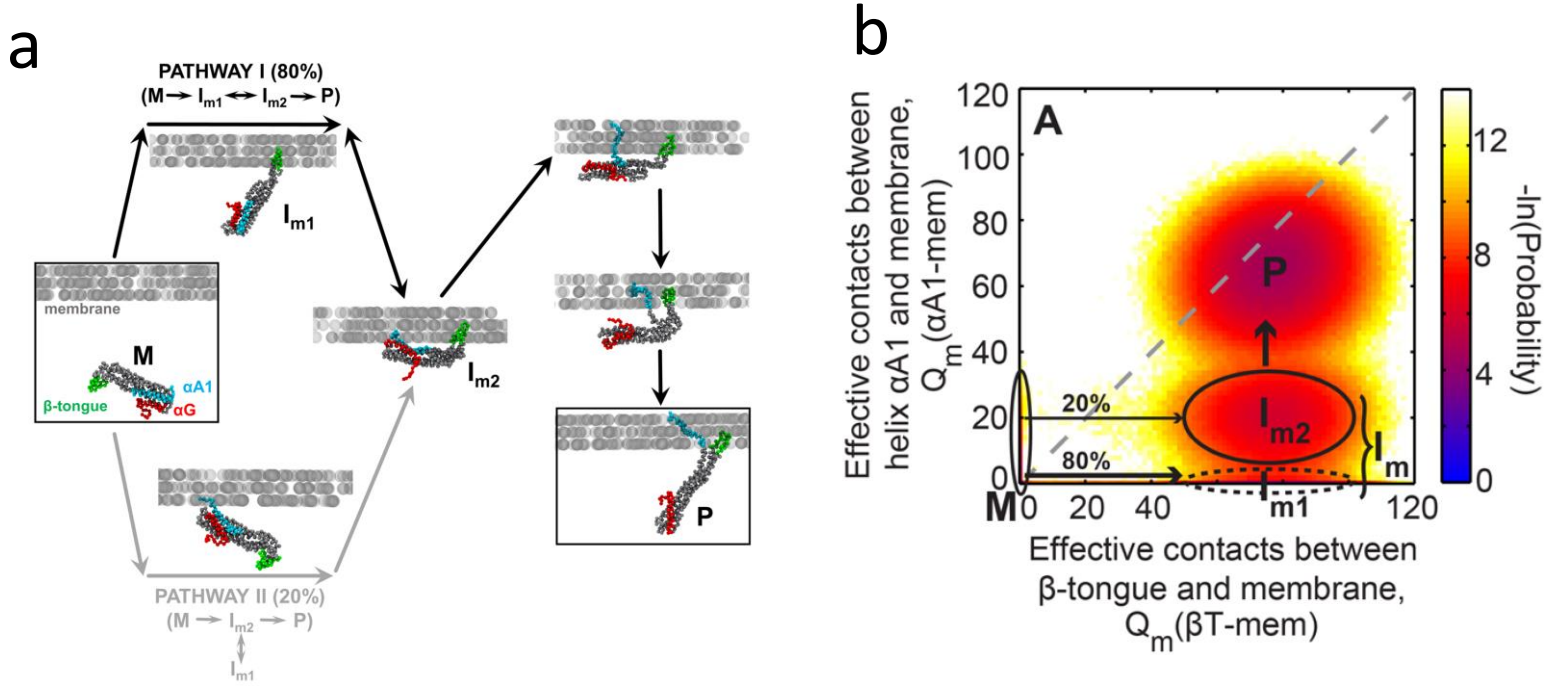

Conformational transition pathways using Structure based models: a) Helix αA1, β-tongue, and helix αG (residues 268−303) are colored cyan, green, and red, respectively. The rest of the protein, and membrane particles are in gray. Pathway I is the major pathway containing two intermediate states I_{m1} (β-tongue bound) and I_{m2} (αA1 bound). In 20 % of instances, initial binding occurred via helix αA1, representing the minor pathway II. These were inferred from analyzing 100 independent replicates of the dual SBM with the membrane b) Probability distribution of the number of contacts formed between helix αA1 and the membrane (Qm(αA1-mem)) vs the number of contacts formed between the β-tongue and the membrane (Qm(βT-mem)) shows the populations of the monomer (M, marked by a vertical ellipse), intermediates I_{m1} and I_{m2} which constitute the Im ensemble together, and the protomer (P).

Fig.5 Single molecule and cholesterol

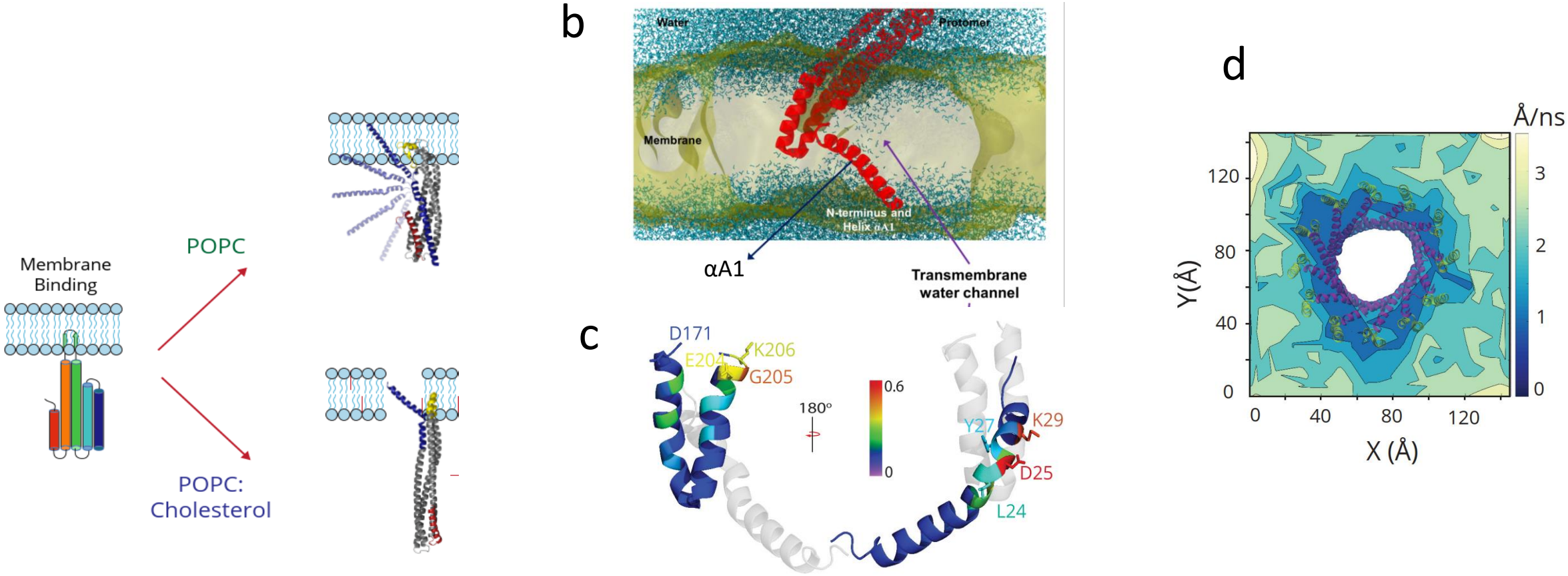

a) Initial interaction of ClyA with membrane is via. β-tongue and diffuses rapidly on membrane (1.1-1.5 $\mu m^2/s$). In the absence of cholesterol, ClyA undergoes rapid switching between the membrane inserted and peripheral conformations *(top).* In presence of membrane cholesterol, molecules undergo complete conversion to membrane inserted state. Presence of cholesterol in the membrane stabilizes the helix αA1 in the membrane which results in significantly lowered mobility on membranes (0.2 $\mu m^2/s$). b) Instantaneous snapshot at 300 ns of the transmembrane protomer from an all-atom MD simulation shows that the protomer structure is stable in POPC membrane. A stable and continuous membrane-spanning water channel is stabilized by the hydrophilic face of the amphipathic transmembrane N-terminal helix. C) Fractional cholesterol occupancy values from MD simulations of the ClyA protomer in POPC-Chol membrane. The residues comprising the CRAC motif are highlighted on the right and high-occupancy residues on β-tongue region are indicated on left d) Snapshots of the cholesterol moiety (yellow, hydroxyl head group in red) in the protomer-protomer interface formed between the β-tongues (two subunits colored in orange and blue) in the two major conformations (left, at 100 ns and right, 300 ns of simulation time) for the ClyA dimer are shown. The residues in cholesterol pocket defined by charged side chains (K206, D171) at the top, a hydrophobic interior (V202, A179, A183) and isoleucine-rich tail (I194, I198) region as well as residue Y27 from the N-terminal helix are highlighted.

Fig.6 –Kinetic models

a

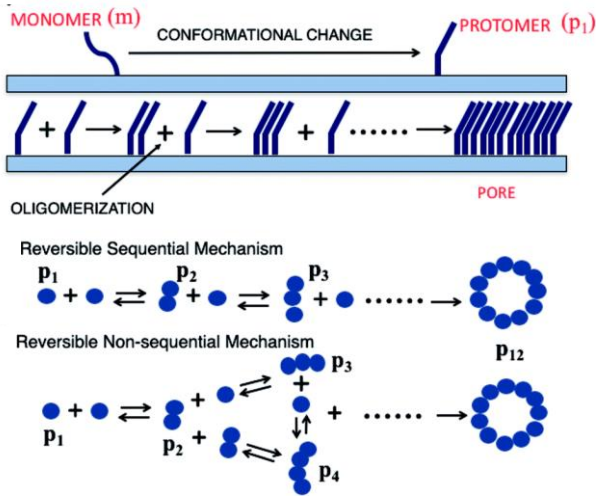

b Erythrocyte lysis

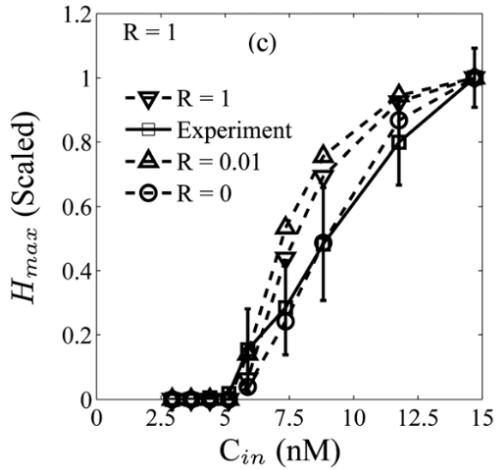

c

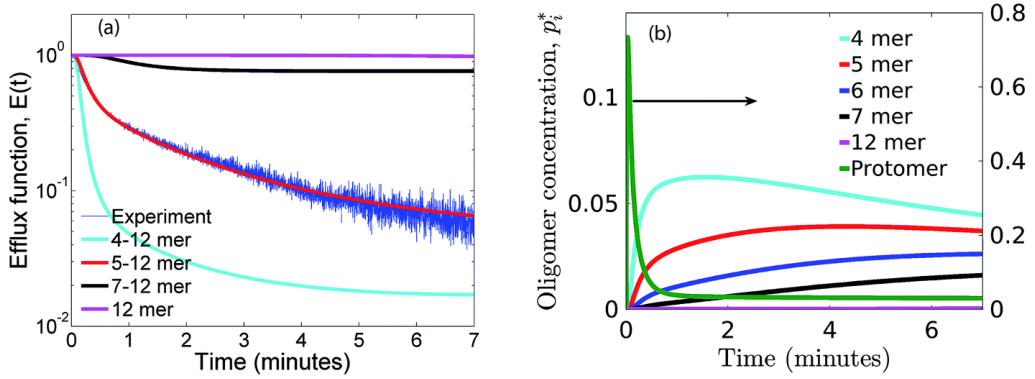

a) Schematic illustrating the key steps of the assembly pathway that are incorporated in the model. The membrane bound monomer first transforms to a protomer and subsequent membrane mediated oligomerization results in the formation of the pore complex. Protomers assemble in a reversible sequential or non-sequential mechanism to form the dodecameric pore complex p_{12}. b) Kinetic model to capture erythrocyte lysis dynamics by Vaidyanathan et al. Here R is ratio of forward and backward time constants of the reversible sequential oligomerization scheme and exhibits a good fit to hemoglobin release data at R=0. c) Predictions from kinetic model by Agrawal et al based on vesicle dye leakage data for the reversible sequential mechanism of oligomerization for various oligomer populations in the efflux function *(left)*. *(right) T*he time evolution of oligomers for optimized parameters corresponding to the 5–12 mer populations for reversible sequential mode.

Fig.7-Transmembrane oligomeric intermediates

a

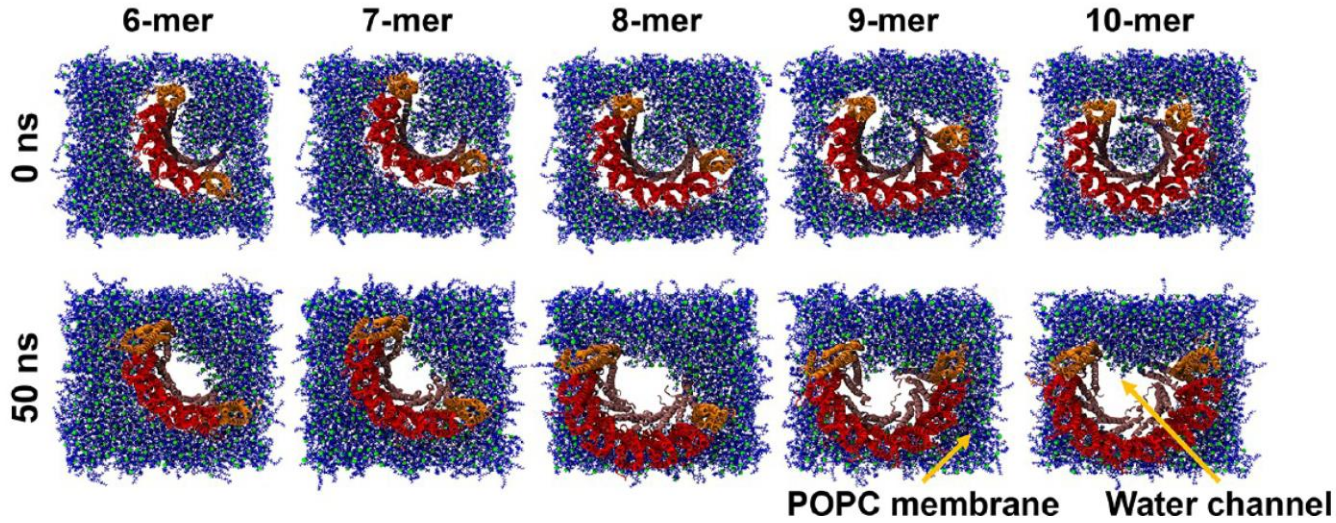

b

Don’t know if we need an image of toroidal lipids here or if we include the pneumolysin PNAS paper water channel as validation?

A) Fully atomistic simulations of ClyA arcs inserted into POPC membranes show rapid lipid evacuation within 50 ns for the 6-mer to the 10-mer (water and ions removed for clarity). The arcs were stably inserted in the membrane for duration of simulation as assessed by RMSD. B)

Fig. 8 : Mitigating ClyA toxicity

a

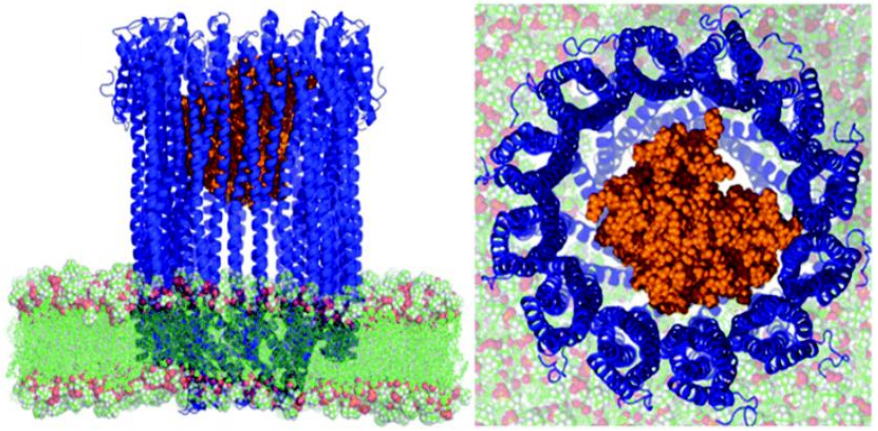

b

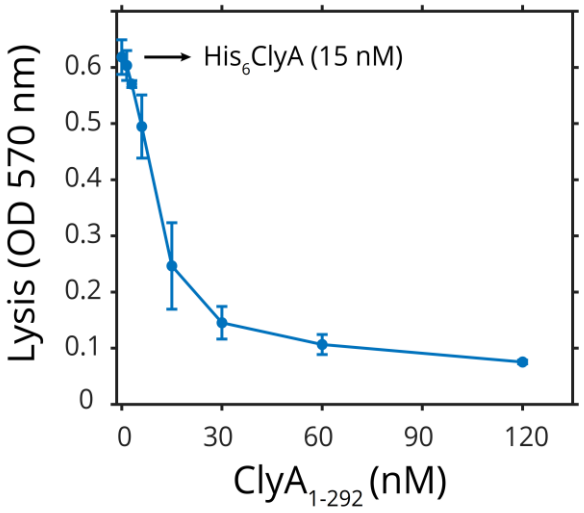

c

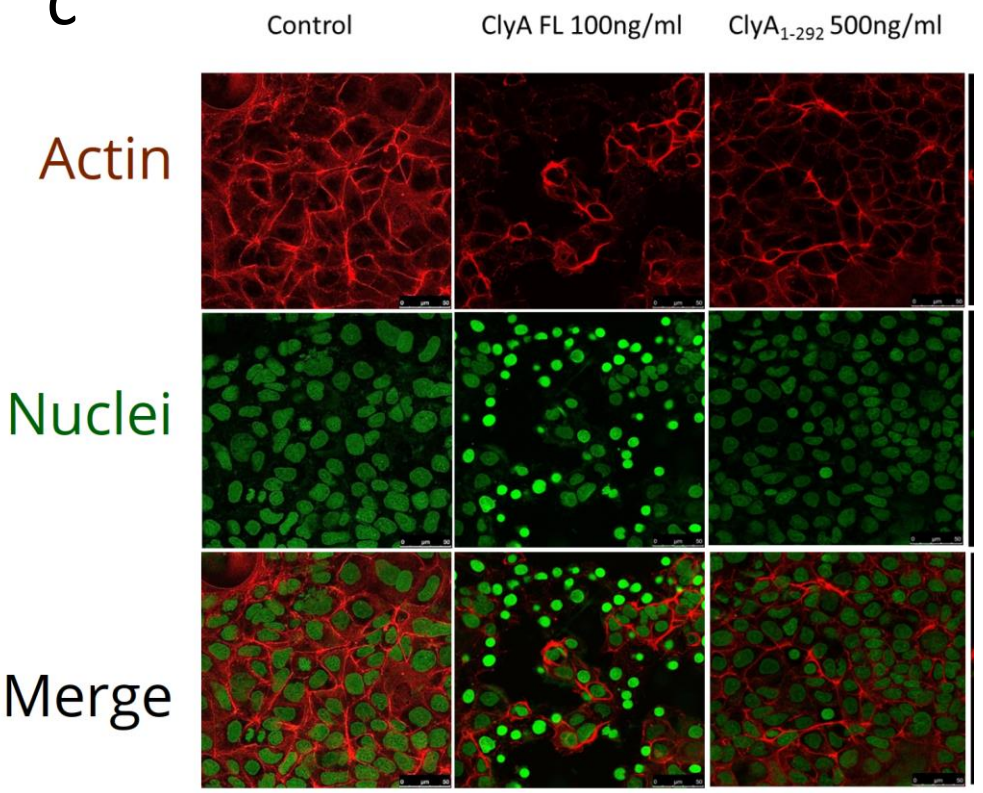

a) Side and top view configurations of ClyA pore in POPC bilayer with Non-protonated PAMAM dendrimer after 200 ns long MD simulations. Efficient blockage b) ClyA (500 ng/ml) was incubated with increasing concentrations of $ClyA_{1-292}$ and hemolysis measured. Incorporation of $ClyA_{1-292}$ units in wild type pores resulted in formation of inactive complexes. C) Caco2 cells incubated with ClyA, $ClyA_{1-292}$ or mixture of the two for 30 minutes at 37°C. Post incubation cells were washed, fixed and stained for actin and nuclei. Disruption of cortical actin observed upon wild type treatment is significantly reduced upon co-incubation with $ClyA_{1-292}$.